Probability density function over the Lorenz attractor: An alternative formulation

R. F. S. Andrade
Instituto de Física, Universidade Federal da Bahia, 40 000 Salvador, Bahia, Brazil
(Received 24 December 1985; revised manuscript received 4 April 1986)

A new method is proposed to evaluate the probability density function ρ over the Lorenz attractor. The conservation statement within the continuity equation for ρ is equivalently replaced by the requirement that all elements of an infinite set of integrals involving ρ are equal. Two approximations for ρ are constructed, after considering a finite number s of such integrals and a function Π depending upon a set of parameters. The values these parameters assume in the approximation for ρ are given by the solution of a system of equations which arises from the requirement that the elements of the subset of s integrals are equal. The results are compared with the probability density function coming from the numerical integration of the continuity equation for ρ.

I. INTRODUCTION

The problem of the determination of the probability density function over the phase space of dissipative systems remains without a general solution both in the transient and the steady states of these systems. The Lorenz model,[1]

$$\begin{aligned}\dot{x}&=\sigma(y-x)\ ,\\ \dot{y}&=-y+rx-xz\ ,\\ \dot{z}&=-bz+xy\ ,\end{aligned}\tag{1}$$

was first proposed to describe the convection of air in the atmosphere. Nevertheless it became the most investigated dissipative system and a large amount of information about its dynamics and the structure of its attractor is now avaliable.[2] With respect to the evaluation of the probability density function ρ over the Lorenz attractor, main results have been reported by Graham and coworkers.[3,4] Their works are based on two fundamental points. The first concerns the opportunity of approximating the Lorenz attractor by two-dimensional invariant manifolds. The second point is the statement of a conservation law (a continuity equation) for ρ over the attractor. This is based on the numerical evidence that all trajectories are trapped by the attractor and remain there. The actual determination of ρ in quoted articles is performed by the numerical integration of the continuity equation we referred to.

The purpose of this work is to develop an alternative method to evaluate the function ρ over the Lorenz attractor. The method is based on a condition which is equivalent to the continuity equation for ρ. It states that all elements of a certain infinite set of integrals $I_k=I_k(\rho,\mathbf{F})$ over the attractor are equal, where $\mathbf{F}=\mathbf{F}(x,y,z)$ indicates the right-hand side of (1). This equivalent condition opens the possibility of finding approximate expressions for ρ, which can be given in terms of functions all over the attractor. To this purpose we consider a tentative function $\Pi=\Pi(y,z;\Lambda)$, where Λ is a set of S parameters λ_l, and a finite number of integrals $I_k=I_k(\rho,\mathbf{F})$, $k=1,2,\ldots,s\le S+1$. The probability density function ρ will be approximated by $\tilde{\rho}(y,z)=\Pi(y,z;\{\lambda_l^*\})$, where the values of λ_l^* come from the solution of

$$I_k(\Pi(y,z;\{\lambda_l^*\}),\mathbf{F})=R=\text{const},\quad k=1,2,\ldots,s\ .\tag{2}$$

If $s=S+1$ the system (2) is completely determined. If $s<S+1$ we have to choose the values of some of the λ_l or the constant value of the right-hand side of (2).

The proposed method demands the use of nonlinear numerical techniques in order to solve the set of s equations. The accuracy of the approximation $\tilde{\rho}$ can be measured either by comparing it directly to ρ, or by comparing average values of functions of the dynamical variables of the system evaluated by direct integration over the attractor with those obtained along a trajectory.

The rest of this paper is organized as follows. Section II gives the details of the construction of the invariant manifolds and how to join them together to approximate the attractor. Also we arrive at the expression for the I_k. In Sec. III we propose an ansatz for the tentative function Π. We present the results we have obtained for $\tilde{\rho}$ after two successive approximations with $s=4$ and 5. Finally we make a critical review of the main steps and difficulties of the proposed method in Sec. IV.

II. THE INVARIANT MANIFOLDS AND THE INTEGRALS I_k

The evaluation of the invariant manifolds consists of finding a relation $x=f(y,z)$ around one of the fixed points of the model[3]: $p_0=(0,0,0)$, $p_\pm=(\pm c,\pm c,r-1)$, $c=\sqrt{b(r-1)}$. We consider the three manifolds M_0, $M_\pm$, which will be written in terms of power series:

$$x=f_*(y,z)=f_*(y_*+\bar{y},z_*+\bar{z})=x_*+\sum_{n=1}^{\infty}A_*^n\Delta^{[n]}\ ,\tag{3}$$

where $*=0,+,-$, A_*^n is a line matrix with 2^n columns, and $\Delta^{[n]}$ is the nth Kronecker power[5] of the vector $\Delta=\binom{\bar{y}}{\bar{z}}$. Each of the manifolds will be determined after inserting (3) into the equation for $\dot{\mathbf{x}}$ in its local form. For instance, we have, in a neighborhood of p_0,

 ©1986 The American Physical Society

$$(-y+rf-zf)\frac{\partial f}{\partial y}+(-bz+fy)\frac{\partial f}{\partial z}=\sigma(y-f)\ , \qquad (4)$$

which gives the values of the A_0^n after comparing the coefficients of equal power of $\Delta^{[n]}$.

The pieces of manifolds constructed by the procedure described above are not bounded. The regions of interest for the approximation of the attractor will be those limited by the boundaries of the attractor. These are obtained by following the trajectories $T^{+(-)}$, which move from a point $p_0^{+(-)}$ of a neighborhood of p_0 along the direction of its unstable one-dimensional manifold to the neighborhood of $p_{-(+)}$. $T^{+(-)}$ generates the boundary of the right (left) branch of the attractor. The different manifolds M_* will be used in the approximation of the attractor in the following way: the region $z \leq 15.5$ will be mapped into M_0. The upper part of the attractor ($z > 15.5$) which encircles the fixed point $p_{+(-)}$ will be mapped into $M_{+(-)}$. The piece of the attractor extends itself until the boundary defined by $T^{+(-)}$. Its left (right) boundary is not defined in the region $15.5 < z < 27$ that corresponds to the region where the two branches of the attractor merge with each other. We want any region of the attractor to be mapped into only one piece of manifold. So when $15.5 < z < 27$, $M_{+(-)}$ will extend itself to the left (right) up to a curve $\tilde{y}^{+}(z)$ [$\tilde{y}^{-}(z)$], which is the locus of the points where it meets $M_{-(+)}$ at a negative (positive) value of y. We will suppose hereafter that $\tilde{y}^{+(-)}$ will consist of two straight line segments linking the points $[-(+)\sqrt{72},27]$ to $[-(+)6.5,17]$ to (0,15.5) (see Fig. 1). We realize that the actual way the two branches of the attractor are glued together for the standard values of the parameters $\sigma=10$, $r=28$, and $b=8/3$ does not differ from the path formed by these line segments substantially.[1,2] Moreover, the possible errors introduced by this hypothesis are not of great importance, since the region under direct influence of this approximation is small in comparison with the rest of the attractor.

The steady-state probability function is given by the continuity equation

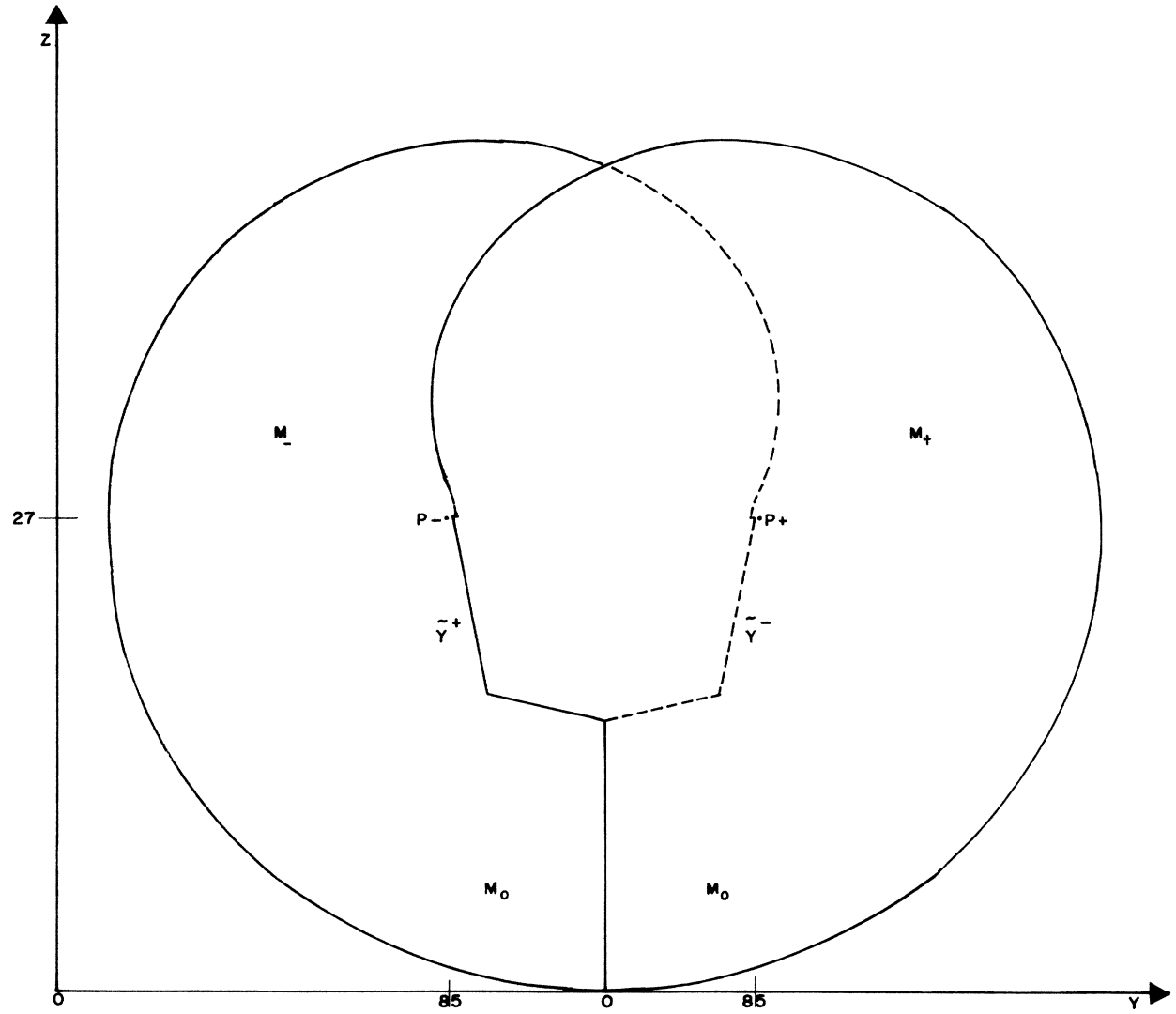

FIG. 1. Lorenz attractor with the indications of the pieces of the several manifolds which approximate it. Note also the curve $\tilde{y}^{+}(z)$ and $\tilde{y}^{-}(z)$, which describes approximately the locus of the phase space where the two branches of the attractor join together.

$$\frac{\partial}{\partial y}(\rho g)+\frac{\partial}{\partial z}(\rho h)=0\ , \tag{5}$$

where g and h stand for $\dot{y}$ and $\dot{z}$. Using the two-dimensional Gauss theorem and a closed Gaussian line formed by two curves which go from the fixed point p_+ to two different points at the boundary T^+, and a third segment linking these two points along the boundary, we come to the result

$$\int_{\omega_+}\rho(y,z)[h(y,z)\cos\theta-g(y,z)\sin\theta]ds=\text{const}\ , \tag{6}$$

where ω_+ is one of the two curves linking p_+ to the boundary, and $\theta=\theta(y,z)$ is the angle between the arc element ds of the curve ω_+ and the positive y direction. As the Gaussian we considered is arbitrary, result (6) is valid for any curve ω_+ of the kind stated above. However, (6) is not valid for a curve linking p_+ to a point on T^-, since Gauss's theorem fails due to the presence of trajectories coming from the negative branch of the attractor. For the same reason the curves ω_+ cannot cross $\tilde{y}^+$ or $\tilde{y}^-$. A similar result is valid for the curves ω_- linking p_- to the boundary T^-. Result (6) asserts that the number of trajectories crossing each ω_+ is conserved, and it can be directly derived from the solution to (5) given in Ref. 4.

III. RESULTS

Now we proceed along the lines described in Sec. I. The I_k in (2) are the integrals (6) along different curves ω_+, henceforth called ω_k. Any tentative function Π which is intended to be an approximation of ρ must enjoy its fundamental properties: to vanish identically at the boundaries of the attractor and at the fixed points, to be bounded, and to be at least continuous and positive definite over the attractor. We will base the definition of our tentative function on an approximation for the function $\rho(y,z)$, which is valid in the region around the origin,[3] which states

$$\rho(yz)\sim(z-c_2y^2)^Q\exp(-u_{20}y^2)\ . \tag{7}$$

In (7), c_2, Q, and u_{20} are functions of the parameters of the model and take the following values for the standard values of σ, r, and b used here:

$$\begin{aligned} &c_2=0.017\,404\,8\ ;\\ &Q=3.435\,396\,3\ ;\\ &u_{20}=0.002\,232\,5\ . \end{aligned} \tag{8}$$

In a neighborhood of p_0 the boundary of the attractor is given by $z\simeq c_2y^2$. Thus Eq. (7) indicates that $\rho\sim(z-z_B)^Q$ when we are close to p_0, where z_B is the point at the lower boundary of the attractor for a fixed value of y. In our ansatz for the tentative function Π, we try to extend the form of the function (7) to the other regions of the attractor far from the origin.

We will restrict ourselves to the evaluation of $\tilde{\rho}_+$, which is the restriction of $\tilde{\rho}$ to that part of the attractor described by M_+ and M_0 ($y>0$). The value of $\tilde{\rho}$ in the other branch of the attractor is obtained from

$$\tilde{\rho}_-(y,z)=\tilde{\rho}_+(-y,z)\ . \tag{9}$$

The total approximate probability density function is

$$\tilde{\rho}(y,z)=\tilde{\rho}_+(y,z)+\tilde{\rho}_-(y,z)\ . \tag{10}$$

Let Z_L^+ and Z_U^+ be the lower and upper boundary of the right branch of the attractor generated by T^+, given as a function of y. Call Y_L^+ and Y_R^+ the left and right part of the same boundary, given as a function of z. The function Z_L^+ will be extended to negative values of y with the help of the boundary generated by T^- in the following way:

$$Z_L^+(y)=Z_L^-(-y),\quad -8.5<y<0\ . \tag{11}$$

We introduce also a second "lower boundary" $\tilde{Z}_L^+(y)$ in the same interval of the definition (11) as the locus of points of the curve $\tilde{y}^+(z)$, defined in Sec. II, given as a function of y. The boundary $Y_L^+(z)$ is not defined in the interval $0<z<27$. So, for use in the definition of Π, we extend the Y_L^+ for values of $z<27$ by

$$Y_L^+(z)=\begin{cases}0, & z<15.5\\ \tilde{y}^+(z), & 15.5<z<27\ .\end{cases} \tag{12}$$

Moreover, we will suppose that the coordinates of the fixed points $p_\pm$ are $(\pm 8.5,27)$ and that $Y_L^+(z\to 27_+)\simeq -8.5$, so that the boundary Y_L^+ with its extention (12) is continuous at $z=27$. This approximation does not have great influence in the determination of $\tilde{\rho}_+$, for its value in the region is negligibly small. On the other hand, the actual form of the boundary Y_L^+ is very difficult to determine and the above simplification helps the definition of the tentative function Π.

Once all different boundaries of the attractor are completely characterized, we define the following functions:

$$p(x,\lambda,X)=|x-X|^\lambda\ , \tag{13}$$

$$q(y,z,\lambda_1,\lambda_4,Y_L^+,Z_L^+,\tilde{Z}_L^+)=\begin{cases}p(y,\lambda_4,Y_L^+), & y>0\\ p(y,\lambda_4,Y_L^+)\left[\dfrac{Y_L^+-y}{Y_L^+}+\dfrac{yp(z,\lambda_1,\tilde{Z}_L^+)}{Y_L^+p(z,\lambda_1,Z_L^+)}\right], & y<0\end{cases} \tag{14}$$

$$u_1(y,z,\lambda_1,\lambda_4,Y_L^+,Z_L^+,\tilde{Z}_L^+)=\begin{cases} q(y,z,\lambda_4,Y_L^+,Z_L^+,\tilde{Z}_L^+), & z>27 \\ \dfrac{z-15.5}{11.5}q(y,z,\lambda_1,\lambda_4,Y_L^+,Z_L^+,\tilde{Z}_L^+), & 15.5<z<27 \\ 0, & z<15.5 \end{cases} \tag{15}$$

$$u_2(y,z,\lambda_2,Y_R^+)=\begin{cases} 0, & z>27 \\ \dfrac{27-z}{11.5}p(y,\lambda_2,-Y_R^+), & 15.5<z<27 \\ p(y,\lambda_2,-Y_R^+), & z<15.5 \end{cases} \tag{16}$$

$$v(y,z,\lambda_3,Y_L^+,Z_U^+)=\begin{cases} 0, & y<|Y_L^+| \text{ or } z>27 \\ \dfrac{(8.5-y)p[z,\lambda_3,Z_U^+(-y)]+(y+Y_L^+)p[z,\lambda_3,Z_U^+(y)]}{8.5+Y_L^+}, & y<8.5 \\ p(z,\lambda_3,Z_U^+), & y>8.5\ . \end{cases} \tag{17}$$

Finally, the function

$$\eta(y,z,\lambda_l,\text{boundaries})$$
$$=p(y,\lambda_2,Y_R^+)p(z,\lambda_1,Z_L^+)$$
$$\times[p(z,\lambda_3,Z_U^+)(u_1+u_2)+vu_2] \tag{18}$$

is the generalization of the first factor of Eq. (7) to all boundaries of the attractor. The apparent complexity in the definition of η is due to the fact that $\tilde{\rho}$ in (10) must be continuous all over the attractor, and the boundaries do jump discontinuously at those points of the attractor where the two branches merge with each other. Also we define two other functions to describe the generalization of the second factor in (7) to the lower part of the attractor and the influence of the fixed points in $\tilde{\rho}$. So let

$$\beta(y,z,\lambda_5)=\begin{cases} 1, & z>27 \\ e^{-\lambda_5 y^2}\left[1-\dfrac{z}{27}\right]+\dfrac{z}{27}, & z<27 \end{cases} \tag{19}$$

and

$$\gamma(y,z,y_+,z_+,\lambda_6,\lambda_7)=[\tanh(\lambda_7\Delta_+)\tanh(\lambda_7\Delta_-)]\lambda_6\ , \tag{20}$$

where

$$\Delta_\pm^2=(y\mp y_+)^2+(z-z_+)^2\ .$$

Finally we define the tentative function Π as

$$\Pi=\Pi(y,z;\lambda_l,\text{boundaries})=A\eta\beta\gamma\ , \tag{21}$$

where A is a normalization constant.

Next we define the curves over the attractor for the evaluation of the I_k: ω_k, $k=1,2,3,4$ are straight lines connecting p_+ to the lower and upper boundary at fixed y and to the left and right boundary at fixed z. ω_5 links p_+ to p_- along a curve which approaches the locus $\tilde{y}^+(z)$ and $\tilde{y}^-(z)=-\tilde{y}^+(z)$ from above.

In a first step we have considered the curves ω_k, $k=1,2,3,4$ to evaluate $\tilde{\rho}_4$. In this case we have put $\lambda_5=0$ always, so that $\beta=1$ all over the attractor. We have chosen different values of R, λ_6, and λ_7 and solved the resulting system (2). The numerical work required to solve (2) may be divided into three major steps: (i) find the value of the I_k; (ii) solve the system with the help of a generalized Newton-Raphson procedure, (iii) find the value of the normalization constant A. To find its value we integrate $\tilde{\rho}_4$ [with $A=1$ in (21)] over the right branch of the attractor and assign this value to $1/2A$. In this last step we also proceed with the evaluation of the moments $\langle x^k y^m z^n\rangle_A=(k,m,n)_A$ using $\tilde{\rho}_4$ as a weight function.

Table I brings the results for some approximations $\tilde{\rho}_4$ which were obtained for different values of R, λ_6, and λ_7. Besides the solution λ_l^*, $l=1,2,3,4$ it brings the value of the normalization constant A, the relative error ϵ_{kmn} of the lowest-order moments $(k,m,n)_A$ with respect to the trajectory-evaluated moments $(k,m,n)_T$, the mean error $\bar{\epsilon}$, and the mean absolute error $\overline{|\epsilon|}$ of the first 43 moments with $k+m+n<6$ and $k+m$ even. The values of the moments depend upon the choice of the free parameters. The first moment $(0,0,1)_A$ is less dependent of that choice and always greater than $(0,0,1)_T$. For some values of the parameters the $\tilde{\rho}_4$-evaluated first 43 moments have a mean absolute error $\overline{|\epsilon|}<2\%$, which is actually very surprising.

Figure 2 brings the curves of different $\tilde{\rho}_4=\tilde{\rho}_{4,+}+\tilde{\rho}_{4,-}$ as well as $\rho=\rho_++\rho_-$ as functions of z for fixed values of y. The curves for $\rho(y,z)$ have been drawn using Ref. 4. Note some characteristics of ρ which are, to some extent, reproduced by $\tilde{\rho}_4$: the height of the curves $y=0$ and $y=16$, the two maxima of the curves $y=4$ and $y=10$ and their relative heights, the form of the curves for $y=0$ and $y=4$ when $z>30$, and so on. However, there are also discrepancies between $\tilde{\rho}_4$ and ρ: $\tilde{\rho}_4$ is always much less than ρ when $y=0$, $y=4$, and $z<20$; $\tilde{\rho}_4<\rho$ for $y=10$ and $y=16$ and $z>30$; the shape of $\tilde{\rho}_4$ shows an irregularity in the region around $\tilde{y}^-(z)$ not present in ρ; the shape of the two maxima of $\tilde{\rho}_4$ in the region about the fixed points is too sharp in comparison with that of ρ.

TABLE I. Solution of the system (41) for $s=4$ and different parametrizations. The value of R does not have great influence in the results and we have kept it constant. However, if it is too small (41) may have no solution. Note that $\lambda_1^*+\lambda_2^*+\lambda_3^*+\lambda_4^*$ is practically constant for all parametrizations. ϵ_{kmn} are given in percent values. $\bar{\epsilon}$ and $\overline{|\epsilon|}$ have been evaluated from the first 43 ϵ_{kmn}. The solution for the system (41) from the third parametrization is not reliable for $\lambda_4^* < -1$ and causes a divergence of $\tilde{\rho}_4$ at the curve $\tilde{y}^+$.

R ($\times 10^{-8}$)	λ_6	λ_7	A ($\times 10^{11}$)	λ_1^*	λ_2^*	λ_3^*	λ_4^*	$\bar{\epsilon}$	$\overline{\lvert\epsilon\rvert}$	ϵ_{001}	ϵ_{200}	ϵ_{020}
1.5	3	0.25	4.6226	3.4473	−0.77722	3.4389	−0.76691	0.573	1.91	2.59	4.84	3.71
1.5	4	0.25	4.5622	3.5723	−0.90281	3.5790	−0.90455	0.292	1.83	2.41	3.77	2.71
1.5	5	0.25	4.4981	3.6916	−1.0219	3.7108	−1.0358	−0.220	1.94	2.23	2.64	1.60
1.5	5	0.30	4.6145	3.4316	−0.76385	3.4255	−0.75072	0.695	1.85	2.58	4.78	3.65
1.5	8	0.30	4.5143	3.6233	−0.95662	3.6400	−0.96224	0.125	1.83	2.30	2.98	1.95
1.5	5	0.35	4.6736	3.2892	−0.62048	3.2645	−0.59404	0.786	2.08	2.78	5.75	4.56
1.5	8	0.35	4.6157	3.4085	−0.74208	3.4023	−0.72582	0.818	1.84	2.58	4.75	3.72
1.5	14	0.35	4.5081	3.6089	−0.94394	3.6271	−0.94717	0.230	1.81	2.29	2.90	1.90

TABLE II. Solution of the system (41) for $s=5$ and the same parametrizations as in Table I. ΔI_5 is the relative error of I_5 evaluated with $\lambda_5=0$ and λ_l^*, $l\leq 4$ as in Table I. Note that $\bar{\epsilon}\simeq -7.5$ is far less than in the first solution. However, ϵ_{001}, is now very close to zero. All absolute values of the λ_l^*, $l\leq 4$ have been reduced and the function $\tilde{\rho}_5$ is less sharp than $\tilde{\rho}_4$.

λ_6	λ_7	A ($\times 10^{11}$)	λ_1^*	λ_2^*	λ_3^*	λ_4^*	λ_5^* ($\times 10^2$)	ΔI_5	$\bar{\epsilon}$	$\overline{\lvert\epsilon\rvert}$	ϵ_{001}	ϵ_{200}	ϵ_{020}
3	0.25	4.2196	3.1472	−0.46332	3.2660	−0.54941	3.6896	−25.8	−7.42	7.42	0.022	−2.58	−3.01
4	0.25	4.1704	3.2694	−0.58648	3.4053	−0.68482	3.6094	−25.6	−7.59	7.59	−0.203	−3.50	−3.85
5	0.25	4.1245	3.3889	−0.70633	3.5377	−0.81610	3.4347	−25.4	−7.89	7.89	−0.307	−4.41	−4.83
5	0.30	4.2137	3.1335	−0.45221	3.2536	−0.53427	3.5701	−25.8	−7.33	7.33	0.015	−2.73	−3.16
8	0.30	4.1355	3.3229	−0.64340	3.4678	−0.74375	3.3818	−25.8	−7.67	7.67	−0.292	−4.21	−4.64
5	0.35	4.2666	2.9964	−0.31376	3.0948	−0.38140	3.5667	−25.6	−7.27	7.27	0.300	−1.79	−2.39
8	0.35	4.2138	3.1108	−0.43101	3.2305	−0.50949	3.5495	−25.8	−7.24	7.24	0.023	−2.74	−3.13
14	0.35	4.1295	3.3089	−0.63128	3.4549	−0.72868	3.3483	−25.8	−7.59	7.59	−0.296	−4.32	−4.73

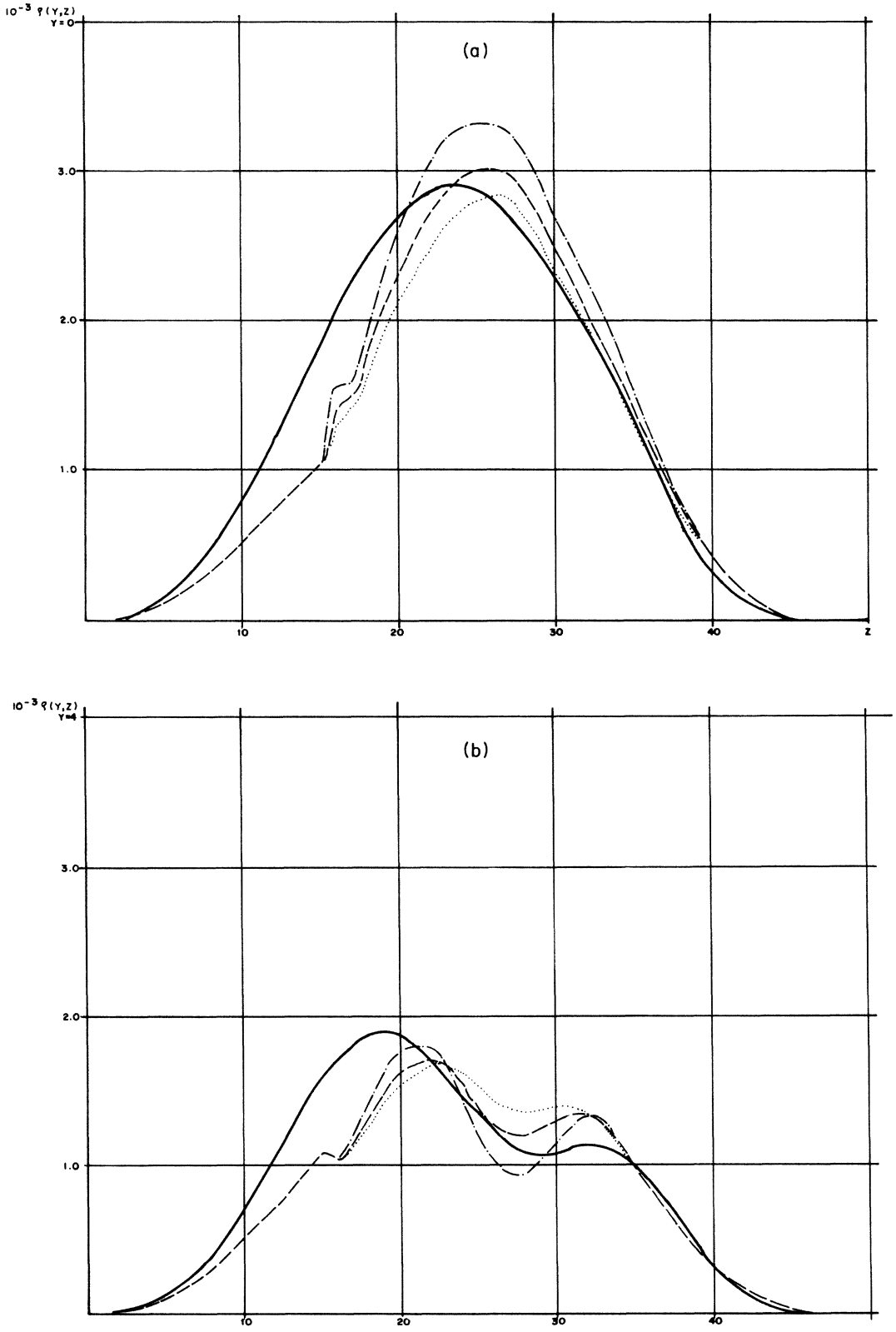

FIG. 2. Comparison of $\rho(y,z)$ (full line) with $\tilde{\rho}_4(y,z)$ at constant values of y, for $R=1.5\times10^8$ and different values for (λ_6,λ_7): — — —, (5,0.30); —·—·—·, (8,0.30); · · ·, (5,0.35). The curves for the three different parameter choices are in practice equal in (d), when $y=16$. The larger the values of λ_1 and λ_3, the sharper the form of $\tilde{\rho}_4$. Note the irregularity of the curves when $\tilde{y}^-$ is crossed at $y=0$ and 4. Best visual accordance is found for the values (5,0.3) of (λ_6,λ_7).

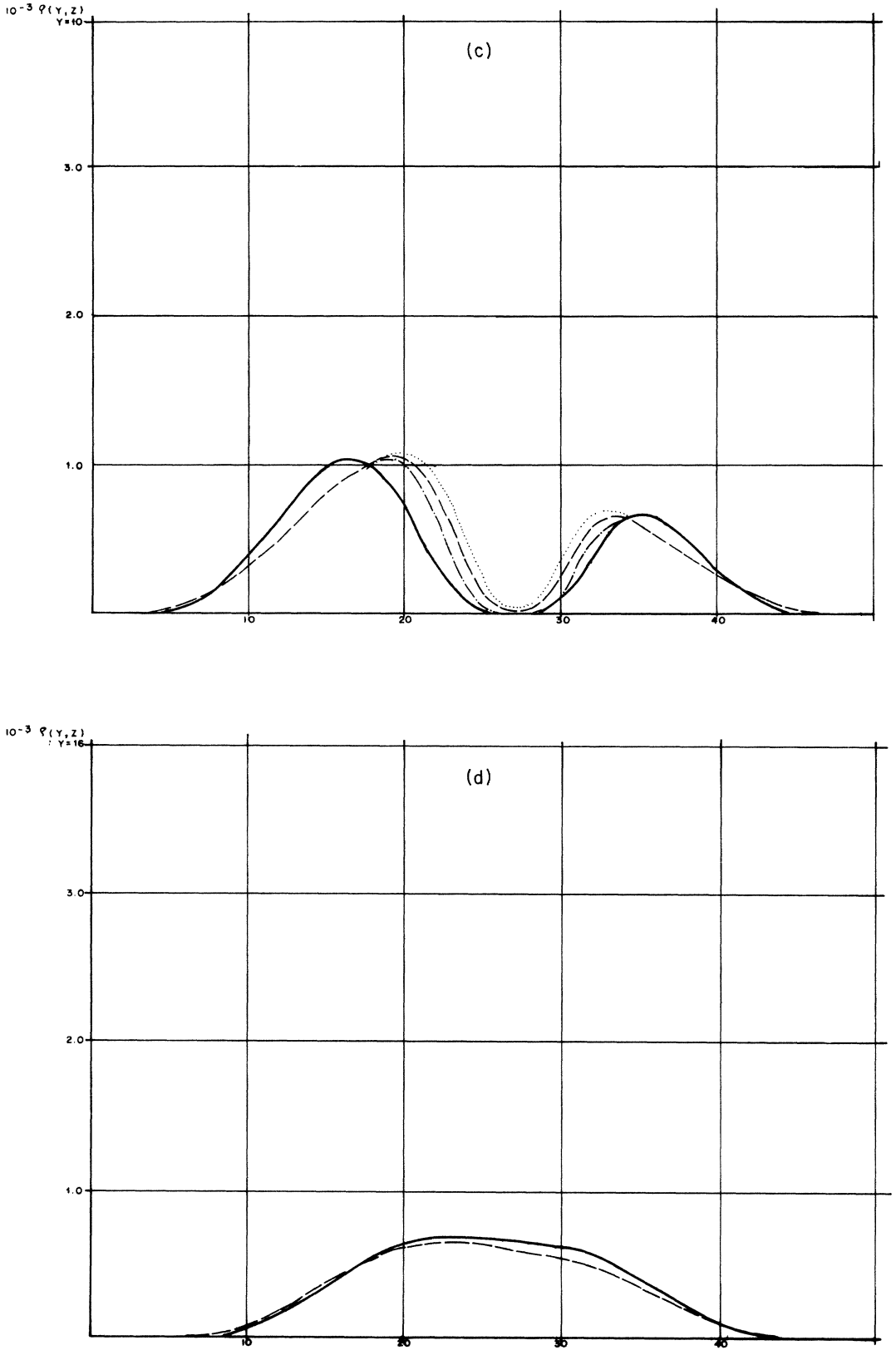

FIG. 2. (*Continued*).

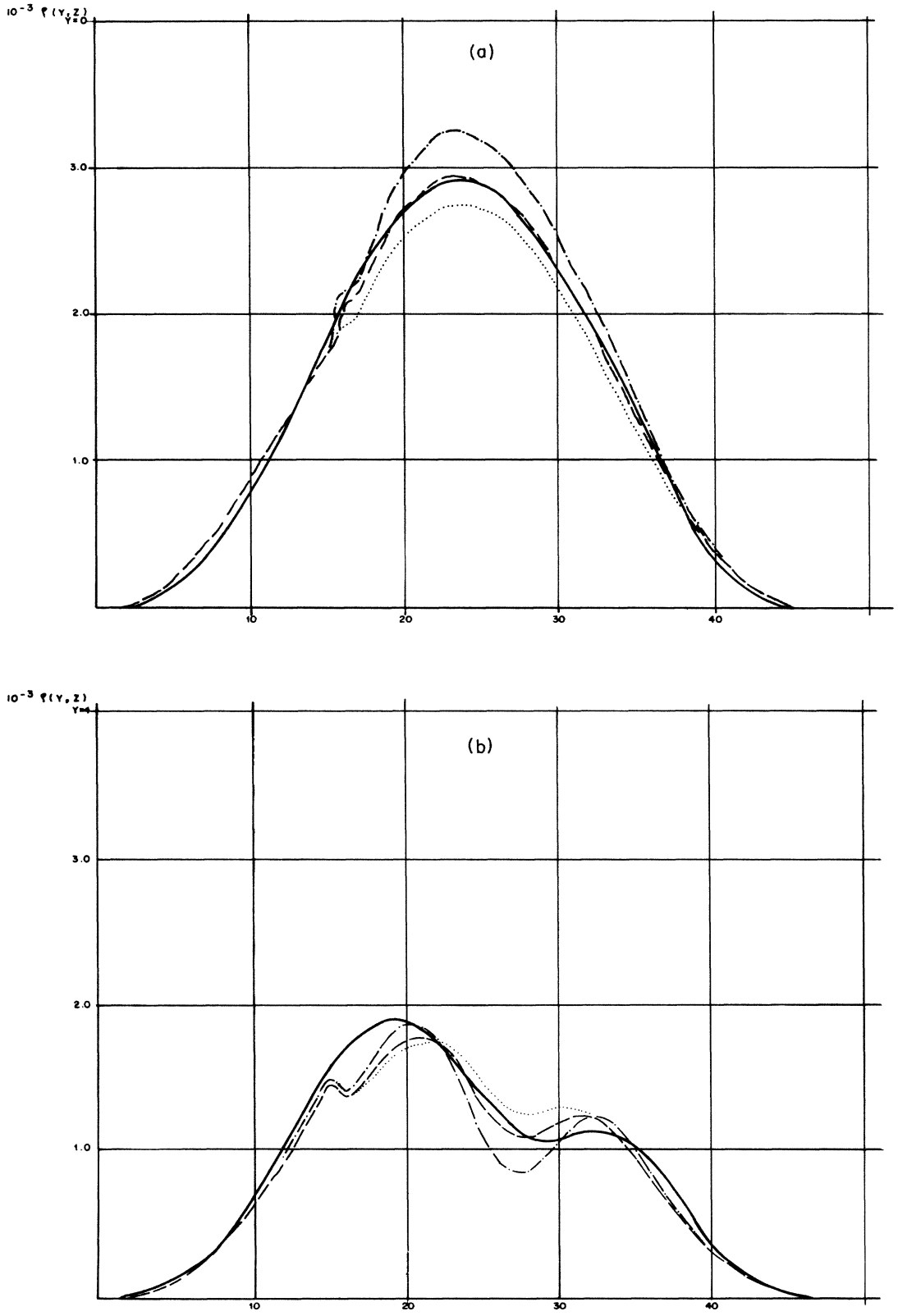

FIG. 3. Comparison of $\rho(y,z)$ with $\tilde{\rho}_5(y,z)$ for the same values of R and (λ_6,λ_7) as in Fig. 2. Note the difference from $\tilde{\rho}_4$ in the regions close to the origin. The curve $y=0$ ($\lambda_6=5$, $\lambda_7=0.3$) fits very well with the exact $\rho(y=0,z)$. The regions far from ρ_0 are those where almost no difference exists between $\tilde{\rho}_4$ and $\tilde{\rho}_5$.

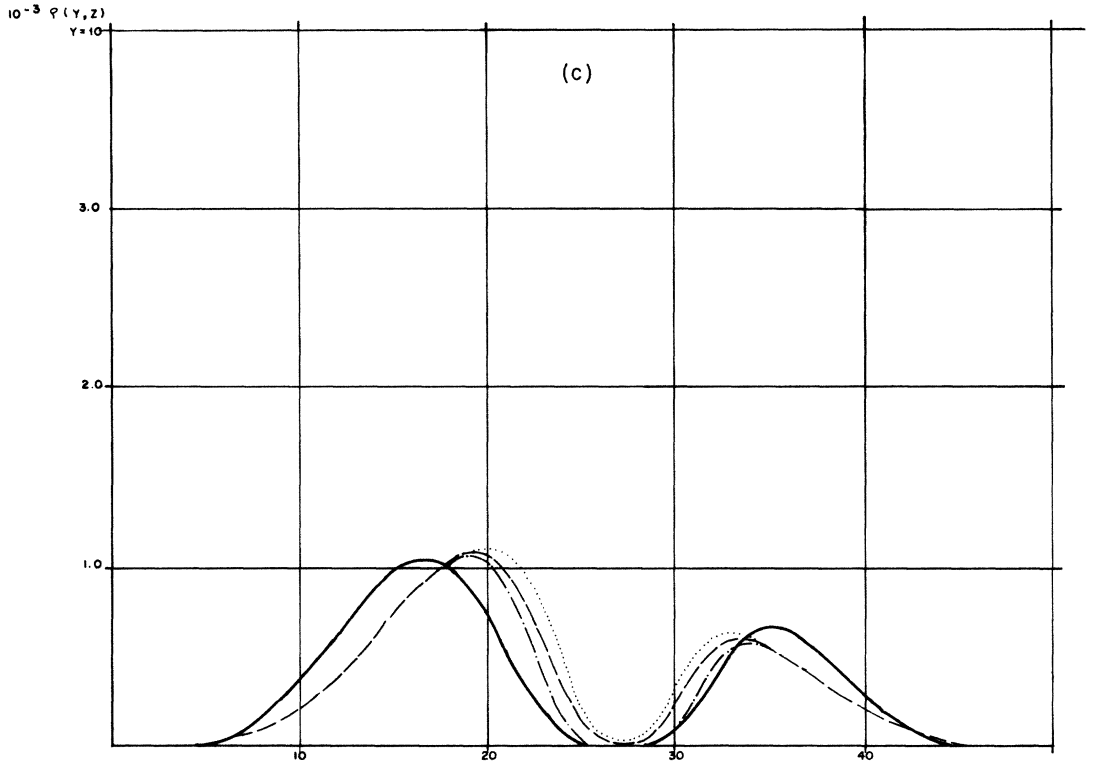

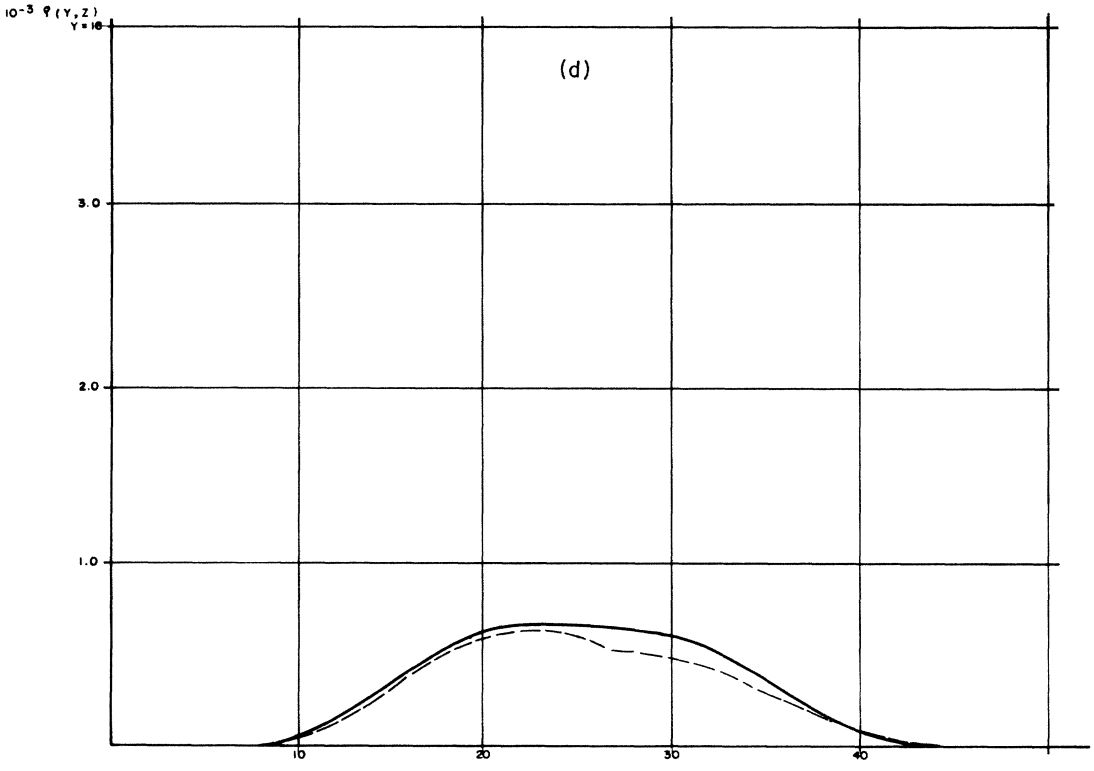

FIG. 3. (*Continued*).

We have considered a higher-order approximation where all the five curves defined previously are taken into account. The fifth unknown of the system is λ_5, while R, λ_6, and λ_7 will remain at our choice as before. The effect of the fifth condition on the approximation will manifest itself in the region close to the curve ω_5, where a better agreement between ρ and $\tilde{\rho}_5$ is expected. Table II shows the results for $\tilde{\rho}_5$. It contains the same entries as Table I, plus the value of λ_5^* and the error in I_5 when it is evaluated with the λ_l^* from the solution of the system with $s=4$ and $\lambda_5=0$. This error ΔI_5 is about 25%, which indicates that $\tilde{\rho}_4$ is too small in that region, as we have pointed out in the discussion of Fig. 2. The results for the ϵ_{kmn}, $\bar{\epsilon}$, and $\overline{|\epsilon|}$ indicate that the function $\tilde{\rho}_5$ is less dependent on the choice of R, λ_6, ad λ_7 as it is expected. We note also that the ϵ_{001} is now closer to zero than in the previous approximation.

In Fig. 3 we draw the function $\tilde{\rho}_5$ for fixed values of y in the same way as in Fig. 2. We note that the function $\tilde{\rho}_5$ has indeed become closer to ρ in the region $y=0$, $y=4$, $y=10$, and $z<20$. The position of the maxima for $y=4$ and of the first maximum for $y=10$ have also improved. The deficiencies for $y=10$, $y=16$, and $z>30$ still remain.

The results in Table II may be compared with the values of Q and u_{20} given by (8). When we are close to p_0 the function $\tilde{\rho}_5$ has the same shape as in (7):

$$\tilde{\rho}_5 \sim |z-Z_L^+|^{\lambda_1+\lambda_2} e^{-\lambda_5 y^2}. \tag{22}$$

We see that $\lambda_1+\lambda_2 \simeq 2.6$ is about 75% of Q, which is a very good result, since this power law is valid for the whole lower boundary. On the other hand $\lambda_5 \simeq 0.03$ stays far away from the value of u_{20}.

IV. DISCUSSION AND CONCLUSIONS

The central idea of the proposed method is very simple. Its major goal is to give an analytical expression which approximates the probability density function ρ all over the Lorenz attractor. However, its implementation faces many difficulties which are due to the particular shape of the Lorentz attractor with its two branches, which requires several manifolds to approximate. These difficulties mask the simplicity of the method. As a matter of fact, the most natural choice for the tentative function, a linear combination of eigenfunctions, cannot be made since a set of such functions over the loci where the pieces of manifolds approximate the strange attractor is not available. We have been forced to take the tentative function Π, whose pointwise definition strongly depends upon the position of each point over the attractor. The requirement that $\tilde{\rho}$ must be continuous has forced us to match different expressions for Π in different parts of the attractor with the help of linear factors such as $(z-15.5)/11.5$ in (15). That particular term gives rise to an unphysical irregularity in the shape of $\tilde{\rho}_4$ and $\tilde{\rho}_5$ in the neighborhood of the straight lines which approximate the place where the two branches merge. Despite these difficulties we have been able to construct approximate expressions $\tilde{\rho}_4$ and $\tilde{\rho}_5$ which display many of the major features of the numerically exact function ρ.

If the condition (6) holds for any curve ω_+, the function $\tilde{\rho}=\Pi(y,z;\{\lambda_l^*\})$ must be equivalent to ρ. If we consider only a finite number of ω_+'s, we expect to get better approximations when the number of curves ω_+ where (6) holds is increased. However, the lack of a complete set of eigenfunctions over the attractor makes it hard to develop a systematic way to get successively better approximations for ρ. If we consider the two approximations $\tilde{\rho}_4$ and $\tilde{\rho}_5$ presented in the previous section, it is hard to decide whether the second approximation is better than the first one. For one side the regions close to ω_5 have experienced a better agreement with the numerically evaluated ρ, as we see from the Figs. 2 and 3. The mean error of the moments, however, which takes into account the value of $\tilde{\rho}$ all over the attractor, has become larger. In our opinion the reasons stated above favors that a better agreement between $\tilde{\rho}$ and ρ will be reached if more curves ω_k and more free parameters are taken into account. The difficulties stated above concerning the further development of the method manifest themselves when we try to bring new free parameters into our tentative function (21). It is not straightforward to decide what new features the new free parameters should describe as well as the way Π should depend on them.

The method relies on heavy numerical work in order to come to the final results. The integrals I_k as well as their derivatives $\partial I_k/\partial\lambda_l$ must be numerically evaluated at each step of the iterative generalized Newton-Raphson procedure to solve the system of equation (we have used NAG-library routine C05PAF). Nevertheless once the solution is found the approximation $\tilde{\rho}$ may be used at any time. The roots of system (2) turned out to be very stable with respect to their numerical evaluation, both when s equals 4 and 5. For a given set of values of the parameters R, λ_6, and λ_7 the root of the system has been reached within 30 iterations, starting from any point. In the best cases we needed 5 iterations to find the λ_l^* with 10^{-5} precision. With respect to the existence of multiple roots of (2), we have failed to find any set of values of the free parameters where more than one root exists.

To conclude, I am aware that any further development of the proposed method depends upon finding a reasonable set of functions to expand the tentative function Π.

[1]E. N. Lorenz, J. Atmos. Sci. **20**, 130 (1963).
[2]C. Sparrow, *The Lorenz Equations: Bifurcations, Chaos and Strange Attractors* (Springer-Verlag, New York, 1982).
[3]R. Graham and H. J. Scholz, Phys. Rev. A **22**, 1198 (1980).
[4]M. Dorfle and R. Graham, Phys. Rev. A **27**, 1096 (1983).
[5]R. Bellman, *Introduction to Matrix Analysis* (McGraw-Hill, New York, 1970).